

Contents lists available at ScienceDirect

### **Materials Letters**

journal homepage: www.elsevier.com/locate/mlblue



# Enhancement of sunlight-induced photocatalytic activity of ZnO nanorods by few-layer MoS<sub>2</sub> nanosheets



Kourosh Rahimi, Mehraneh Moradi, Roghayeh Dehghan, Ahmad Yazdani\*

Tarbiat Modares University, Department of Basic Sciences, Tarbiat Modares University, Tehran, Iran

#### ARTICLE INFO

Article history: Received 28 August 2018 Received in revised form 13 September 2018 Accepted 18 September 2018

Keywords:
Few-layer molybdenum disulfide
Zinc oxide nanorods
Photocatalyst
Band diagram
Composite materials
Nanoparticles

#### ABSTRACT

Few-layer exfoliated  $MoS_2$  nanosheets were easily composited with ZNO nanorods. It was found that  $MoS_2$  nanosheets could enhance the sunlight-induced photocatalytic activity rate of ZNO by 74%. In addition, we showed that under UV-blocked sunlight irradiation,  $MoS_2$  weakens the photocatalytic activity rate of ZNO by 33%. Finally, we discussed the mechanisms behind the enhanced (weakened) photocatalytic activity under sunlight (UV-blocked sunlight) irradiation based on the UV-VIS absorption and photoluminescence spectra as well as the potential band diagrams of the  $ZNO/MoS_2$  composite.

© 2018 Elsevier B.V. All rights reserved.

#### 1. Introduction

Under light irradiation, some metal-oxide semiconductors are able to catalyze reduction-oxidation reactions, known as photocatalysis, both for hydrogen production and degradation of organic materials [1]. In particular, ZnO, as an n-type semiconductor (3.37 eV), is a promising photocatalyst that can be easily synthesized in various nanoscale morphologies [2,3]. For example, ZnO nanorods, as a one-dimensional structure, show a stronger photocatalytic activity than that of spherical nanoparticles, which results from their dimensional anisotropy and higher aspect ratio [4]. However, due to its wide bandgap and the high recombination rate of its photogenerated charge carriers, ZnO has a limited photocatalytic activity under the visible light irradiation.

One way to deal with the limitations of metal-oxide photocatalysts is to design heterojunction-based photocatalysts that have a higher photocatalytic activity because they can spatially separate the photogenerated electron-hole pairs [5,6]. Because of its relativity narrow bandgap, which varies depending on the number of its layers, MoS<sub>2</sub> can absorb the visible region of sunlight. Due to its unique layered structure and relatively narrow and adjustable p-type bandgap, MoS<sub>2</sub> sheets can be combined with ZnO to form a heterojunction (staggered) photocatalyst, lower its bandgap,

enhance its absorption in both UV and visible regions, increase its ability to separate photogenerated electrons and holes, and act as a host to absorb target molecules [7-12].

Here, few-layer MoS<sub>2</sub> sheets were composited with ZnO nanorods to enhance their sunlight-induced photocatalytic activity. Finally, the mechanism behind the role of MoS<sub>2</sub> in the enhancement was discussed based on the possible energy band diagrams in different wavelength regions.

#### 2. Experimental methods

Few-layer MoS<sub>2</sub> nanosheets were exfoliated from bulk MoS<sub>2</sub> powder based on the work of Yao et al. [13]. First, 100 mg MoS<sub>2</sub> powder (Sigma-Aldrich, 99%) was mixed in 0.5 ml acetonitrile (Merck, 99.9%) and it was ground for 1 h. The obtained powder was mixed in a 45 vol% ethanol/water solvent, and it was tipsonicated (200 W, 60 min) for 1 h to be exfoliated. The well-known thermal decomposition of zinc acetate powder was applied to synthesize ZnO nanorods. First, 1 g zinc acetate dihydrate (Zn (O<sub>2</sub>CCH<sub>5</sub>)<sub>2</sub>(H<sub>2</sub>O)<sub>2</sub>) (Merck, 99.5%) was heated in a crucible at 300 °C for 3 h to be thermally decomposed into zinc oxide nanorods. Finally, the obtained powder was washed with ethanol and deionized water. To prepare the ZnO/MoS<sub>2</sub> composite, 20 mg of the synthesized ZnO nanorod powder was mixed into 10 ml of the synthesized MoS<sub>2</sub> suspension in an ultrasonic bath for 30 min and by stirring for 2 h. The obtained mixture was dried at 70 °C

<sup>\*</sup> Corresponding author.

E-mail address: yazdania@modares.ac.ir (A. Yazdani).

in a vacuum oven for 12 h and subsequently, it was heated at 200  $^{\circ}\text{C}$  for 2 h.

Photocatalytic degradation of 50 ml of  $2.5 \times 10^{-5}$  M methylene blue (MB) dye was monitored based on the dye decolorization by measuring the MB solution absorbance at 665 nm with 20 mg of each powder sample. The mixture was kept for 1 h in the dark to achieve its surface adsorption-desorption equilibrium. To simulate the sunlight as the light source, a 250 W metal-halide lamp (Philips, ~1000 W/m<sup>2</sup>) was used. In some tests, a camera UVblocking filter was used to analyze UV-blocked-sunlight-induced photocatalytic activities of the samples. A water circulator was used to maintain the reactor temperature at room temperature  $(\sim 25 \, ^{\circ}\text{C})$  in order to eliminate possible thermal effects. The reported values are the averages of three tests. We fitted on the obtained time-varied photocatalytic activity data the pseudofirst-order Langmuir-Hinshelwood kinetics [14].  $-\text{Ln}(C_t/C_0) = kt$ . where C<sub>t</sub> is the concentration of MB at time t and k is the rate constant of the degradation reaction.

The following instruments were employed for characterizations: FESEM (Hitachi S-4160), X-ray diffractometer (X'Pert MPD, Philips,  $\lambda$  = 1.5406 Å), AFM (Veeco Autoprobe CP-research) working in contact mode with a Si tip of 10 nm curvature radius in the air, UV–Vis spectrophotometer (Unico, 4802), PL spectrophotometer

(Gilden p  $\lambda$  otonics). Bandgap energies of the samples, as semiconductors, were determined from their UV–Vis absorption spectra based on the Tauc relation,  $h\nu = A(h\nu - E_g)^n$ , where h is the Plank constant,  $\nu$  is the frequency of incident light, A is the absorbance,  $E_g$  is the bandgap, and n is a constant that depends on the nature of the bandgap (1/2 for direct bandgaps).

#### 3. Results and discussion

Fig. 1(a and b) shows a FESEM image and an AFM micrograph of the exfoliated MoS<sub>2</sub> sheets. As it is seen, there are several overlapping sheets, which are relatively wide. According to the height profile shown in Fig. 1(b), the thickness of each MoS<sub>2</sub> sheet is about  $\sim$ 3–4 nm. It is seen in the inset of Fig. 1 (a) that there is only a weak (0 0 2) peak at  $2\theta$  = 14.3° in the XRD pattern of the exfoliated MoS<sub>2</sub> without other peaks related to the bulk MoS<sub>2</sub>, which suggests that the exfoliated MoS<sub>2</sub> is few-layer. A FESEM image of the synthesized ZnO nanorods is shown in Fig. 1(c), where their diameter is  $\sim$ 100 nm, and their length is in the range 0.1–1  $\mu$ m. An XRD pattern of the synthesized ZnO nanorods is shown in the inset of Fig. 1 (c), where all peaks are matched with the hexagonal wurtzite phase of the JCPDS Card No. 01–079–0208, without other impurity

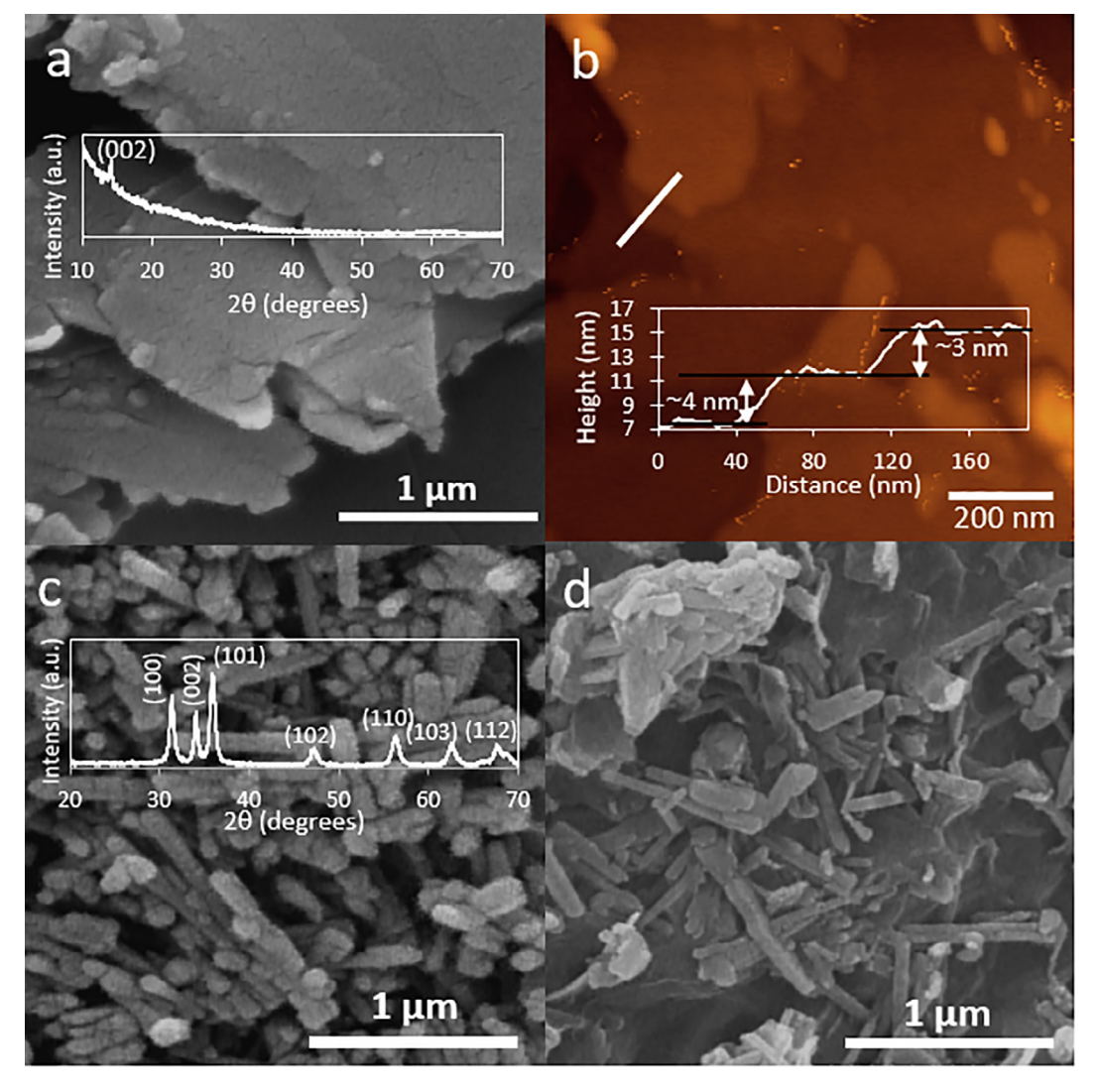


Fig. 1. (a) FESEM image, XRD pattern (inset) and (b) AFM micrograph of the exfoliated MoS<sub>2</sub> on a mica substrate. (c) FESEM image and XRD pattern (inset) of the synthesized ZnO nanorods and (d) FESEM image of the prepared ZnO/MoS<sub>2</sub> composite.

## Download English Version:

# https://daneshyari.com/en/article/10156062

Download Persian Version:

https://daneshyari.com/article/10156062

<u>Daneshyari.com</u>